· Article · Advances in Polar Science
doi: 10.13679/j.advps.2019.3.000xx September 2019 Vol. 30 No. 3: xx-xx

Interaction of diabatic processes, large-scale eddies and the mean atmospheric circulation over the Atlantic, Arctic and Eurasia

Ralf JAISER*, Dörthe HANDORF & Klaus DETHLOFF

Alfred-Wegener-Institut, Helmholtz-Zentrum für Polar- und Meeresforschung, Telegrafenberg A45, 14473 Potsdam

Received 30 April 2018; accepted 14 January 2019

Abstract In the last decade, the atmospheric part of the climate system experienced a shift from pronounced zonal to stronger meridional flow configurations and regionally diverse changes and trends. The climate system shows complex interactions and nonlinear behavior, manifested in global warming, rising ocean temperatures and the retreat of Arctic sea ice. Although atmospheric trends and changes are observed, underlying processes are not well understood. In this study we diagnose the interaction of large-scale atmospheric eddies and the mean flow with respect to diabatic heating and cooling processes that impact on the atmospheric advection of heat. For this purpose, the three-dimensional Eliassen-Palm flux theory is used in combination with an analysis of the thermodynamic equation, diabatic heating and cooling and heat advection. The most recent decades of observed winter climate are evaluated in terms of climatology and trends over the Atlantic, Arctic and Eurasia. The change of the atmospheric circulation and related processes differ between early and late winter. In early winter, the interaction of macro-turbulent eddies with the mean flow is inhibited at the Atlantic jet stream entrance region and atmospheric heat is meridionally advected into the Arctic, both related to strong high pressure anomalies. In late winter, these anomalies are inverted and a negative phase of the Arctic Oscillation with a more wavy mean flow and a tendency towards stronger meridionalization is observed.

Keywords **diabatic heating, heat advection, wave-mean flow interactions, North Atlantic Oscillation, Arctic Oscillation, sea ice, climate change, Arctic Amplification, polar-mid-latitude linkages**

Citation: Jaiser R, Handorf D, Dethloff K. Interaction of diabatic processes, large-scale eddies and the mean atmospheric circulation over the Atlantic, Arctic and Eurasia. Adv Polar Sci, 2019, 30(3): xx-xx, doi: 10.13679/j.advps.2019.3.000xx

1 Introduction

Climate changes in the Atlantic and Eurasian sector have been exposed to regional and global drivers and are characterized by strong trends. Generally, CO_2 levels are rising globally and climate is subject to global warming. Sea level temperatures (SST) are rising and a change to a positive phase of the Atlantic Multidecadal Oscillation (AMO) is observed for recent decades. Furthermore, sea-ice extent is rapidly declining in the Arctic. From the perspective of the atmospheric circulation, these processes are external drivers having the potential to induce trends in the atmospheric circulation.

Global climate change is a phenomenon that is not only related to CO_2, but also to several other anthropogenic influences on the whole climate system as reviewed by the Intergovernmental Panel on Climate Change (Pachauri et al., 2014). These changes do not lead to a uniform global warming, but involve changes in atmospheric dynamics, circulation changes and regional differences. Furthermore, SST and sea-ice changes are related to global climate change and potentially interact with each other. For instance, the atmospheric response to changes of sea ice and CO_2 is

* Corresponding author, E-mail: ralf.jaiser@awi.de

mostly additive (McCusker et al., 2017), while the response to sea ice loss varies depending on the state of the AMO (Osborne et al., 2017).

Changes in the AMO phase and corresponding changes in the North Atlantic SSTs affect European climate. The effects of SSTs are expected to be small compared to internal variability (Kushnir et al., 2002). While the short term variations of European SAT are dominated by the North Atlantic Oscillation (NAO) variability, long term variations can be related to SST anomalies (Årthun et al., 2018). Nevertheless, Gastineau and Frankignoul (2015) find negative phases of the NAO in winter related to a warm AMO phase. Therefore, a wide variety of potential influences of North Atlantic SST anomalies on the northern hemisphere climate exist on time scales from seasons to multiple decades (i.e. Grosfeld et al., 2008; Arguez et al., 2009; Gámiz-Fortis et al., 2011; Gan and Wu, 2015). Thus, observed trends in SST very likely lead to trends in the atmospheric circulation. Here, diabatic processes play a role especially in winter, when the ocean acts as a heat source.

The impact of Arctic sea-ice decline and Arctic Amplification on the atmospheric circulation in winter is one of the hot topics in climate sciences. A particular interest is the analysis of linkages between the Arctic and mid-latitude climate. It has been addressed in a variety of controversial studies discussing mechanisms, processes, impacts and the significance in observations and models (Cohen et al., 2014; Vihma, 2014; Barnes and Screen, 2015; Overland et al., 2015, 2016; Francis, 2017; Screen et al., 2018). In these studies, the most discussed finding is that sea-ice reduction leads to a signal similar to a negative phase of the Arctic Oscillation (AO) or NAO with reduced meridional temperature and pressure gradients and consequently reduced zonal winds in mid-latitudes and continental cooling in winter. The highest potential for a robust connection exists between Barents-Kara sea ice and Siberian cold anomalies (Zhang et al., 2018). Two main pathways of explanation for these kinds of linkages exist. The first pathway works in the troposphere alone. Arctic warming related to reduced sea ice directly decreases the temperature and pressure gradient (Francis and Vavrus, 2012; Tang et al., 2013; Semmler et al., 2016). Further amplification of this mechanism arises from warming events impacting the winter surface temperatures in the central Arctic that have positive trends (Graham et al., 2017). Additional heat release at the surface from the ocean to the atmosphere also leads to changes in vertical stability affecting atmospheric baroclinicity. Consequently, synoptic-scale systems in the Arctic are observed more often and with higher intensity (Stroeve et al., 2011; Jaiser et al., 2012; Rinke et al., 2017). It is indicated by Crasemann et al. (2017) that this applies preferably to the early winter season. The second pathway involves the stratosphere. Changing tropospheric patterns lead to enhanced planetary wave activity disturbing the stratospheric polar vortex in winter. Weak vortex anomalies propagate back into the troposphere leading to negative AO-like anomalies (Jaiser et al., 2013, 2016; Kim et al., 2014; Kretschmer et al., 2016). Both, the tropospheric and stratospheric pathways are coupled in the troposphere and mutually intensify the impact. The complexity is further enhanced by Eurasian snow anomalies that impact the system in similar ways through the stratospheric pathway (Cohen et al., 2007; Fletcher et al., 2009; Liu et al., 2012; Peings et al., 2012; Furtado et al., 2016; Gastineau et al., 2017; Tyrrell et al., 2018). These snow anomalies are potentially linked to Arctic changes in terms of additional moisture sources and changed transports by baroclinic cyclones (Wegmann et al., 2015). Snow and sea-ice anomalies relate to the atmosphere through diabatic processes in terms of changing heat sources and sinks at the surface.

It is important to note that a trend of more negative NAO/AO phases and continental cooling in recent winters is not well reproduced by climate model simulations. Smith et al. (2017) showed that not only sea-ice changes are important but also different background states. They find a positive NAO response as well as a negative NAO response in winter. Crasemann et al. (2017) detected a higher frequency of negative NAO situations related to less sea ice extent only in late winter. Thus, there is a potential for intraseasonal variability, which will be further analyzed in this study. Overall, amplified changes in the Arctic characterized by strong trends in sea ice, snow and surface conditions are potential candidates for explaining trends in the atmospheric circulation such as observed trends to a more pronounced negative NAO/AO in winter.

While potential drivers for impacts on the large-scale atmospheric circulation exist, the underlying processes are not well understood. The large-scale circulation can be described by the mean atmospheric flow interacting with large-scale eddies, connected with planetary-scale and synoptic-scale processes. The zonal mean theory of interactions between large-scale eddies and the mean flow is based on Andrews and McIntyre (1976) and Edmon et al. (1980), showing that the zonal mean wind tendency is forced by the divergence of momentum and heat fluxes. With the work of Hoskins et al. (1983), Plumb (1985, 1986), Trenberth (1986) and Dethloff et al. (1987) this concept has been extended to the three-dimensional time-averaged flow, allowing the three-dimensional discussion of the interaction between large-scale eddies and the mean flow. Diabatic processes in terms of sources and sinks of energy play an important role in these three-dimensional interactions, which we analyzed via the thermodynamic energy equation following Trenberth and Smith (2009). A combined analysis of diabatic processes in relation to interactions between eddies and the mean flow has the potential to improve our dynamical understanding of the underlying atmospheric processes.

In this study, we focus on the discussion of climatologies and trends from 1979 to 2016 in the Atlantic,

Arctic and Eurasian sector. The focus is on the three-dimensional interaction between large-scale eddies and the mean flow, their relation to diabatic heating and cooling processes and the atmospheric circulation. The aim is to develop and implement an improved framework of diagnostics for a better and more detailed understanding of atmospheric processes, dynamics and related changes. For this purpose, we rely on the above mentioned concept and implement the three-dimensional Eliassen-Palm (EP) flux theory in combination with an analysis of the thermodynamic equation and heat advection. In the following section we introduce the methods. Afterwards the main results are presented and discussed in detail.

2 Methods

This study explores the thermodynamic equation in the perspective of the atmospheric heat energy budget based on Trenberth and Smith (2009). The diabatic heating source $\dot{Q}$ is in balance with the local temperature change and advection of heat in the atmosphere.

$$\dot{Q} = c_p \left(\frac{\partial}{\partial t} T + \boldsymbol{v}_\mathrm{h} \cdot \nabla T + \omega \left(\frac{\partial}{\partial p} T - \frac{R}{c_p} \frac{T}{p} \right) \right) \tag{1}$$

Here, c_p is the specific heat capacity for constant pressure, T is the temperature, v_h is the horizontal wind vector (u, v), ω is the pressure tendency (vertical wind in pressure coordinates), R is the gas constant and p is the atmospheric pressure. Equation (1) is time-averaged and transformed to the flux form by using the continuity equation and further simplified by using the hydrostatic approximation $\partial\Phi / \partial p = -RT / p$:

$$\overline{\dot{Q}} = c_p \left(\frac{\partial}{\partial t} \overline{T} + \overline{v_\mathrm{h}} \cdot \nabla \overline{T} + \overline{\omega} \frac{\partial}{\partial p} \overline{T} + \nabla \cdot \overline{\boldsymbol{v}_\mathrm{h}' \boldsymbol{T}'} + \frac{\partial}{\partial p} \overline{\omega' T'} \right) + \overline{\omega} \frac{\partial}{\partial p} \overline{\Phi} + \overline{\omega' \frac{\partial}{\partial p} \Phi'} \tag{2}$$

An overline indicates the time mean, while the prime stands for the deviation from that mean. In this study the time mean corresponds to monthly averages and the deviations are calculated as differences from that mean without any further filtering. The mean diabatic heating rate $\overline{\dot{Q}}$ can be estimated as a residual based on Equation (2). The right-hand side of the equation will be discussed in three separate parts:

$$\overline{\dot{Q}}_\mathrm{tend} = c_p \frac{\partial}{\partial t} \overline{T} \tag{3}$$

$$\overline{\dot{Q}}_\mathrm{turb} = c_p \left(\nabla \cdot \overline{v_\mathrm{h}' T'} + \frac{\partial}{\partial p} \overline{\omega' T'} \right) + \overline{\omega' \frac{\partial}{\partial p} \Phi'} \tag{4}$$

$$\overline{\dot{Q}}_\mathrm{mean} = c_p \left(\overline{v_\mathrm{h}} \cdot \nabla \overline{T} + \overline{\omega} \frac{\partial}{\partial p} \overline{T} \right) + \overline{\omega} \frac{\partial}{\partial p} \overline{\Phi} \tag{5}$$

The turbulent advection $\overline{\dot{Q}}_\mathrm{turb}$ (4) contains all flux terms and thus deviations from the time average. The mean advection $\overline{\dot{Q}}_\mathrm{mean}$ (5) contains the remaining time mean terms. The tendency term $\overline{\dot{Q}}_\mathrm{tend}$ (3) is formed by the local time derivative of temperature corresponding to the intraseasonal temperature change. It is an order of magnitude smaller than all other contributions. Furthermore, the focus of this study is on circulation changes and the interaction between large-scale eddies and the time-mean flow, and therefore the tendency term is omitted in the discussion.

The mean diabatic heat source is in balance with turbulent and mean heat advection only, if small local temperature changes are omitted. Therefore, only these three terms can interact. Advection is related to the transport of heat from or to sources and sinks, respectively. Here, positive advection corresponds to a gain of heat of the atmospheric flow and thus a transport away from the source. Drivers of heat sinks and sources are radiative processes as well as interaction with kinetic and latent energy components, which are not discussed here. Additionally, the mean and turbulent advection are also able to interact meaning that heat can be exchanged between these two scales of motion. In the framework of this study, mean heat advection is related to the quasi-stationary mean flow, while turbulent advection is related to atmospheric eddies on large scales ranging from synoptic-scale systems to planetary scales. A discussion of differences between synoptic scales and planetary scales of the large-scale turbulent advection is enclosed as supplementary material.

We use EP flux diagnostics to characterize the interaction between large-scale turbulence and the mean flow. Since we are interested in regional relations in comparison to the heat advection terms, we use the three-dimensional or local EP flux formulation by Trenberth (1986). The forcing of the time-mean zonal wind is described by the divergence of the EP flux vector in spherical log-pressure coordinates (λ, ϕ, z).

$$\nabla \cdot E = \frac{1}{r_E} \frac{\partial}{\partial \lambda} \left(\overline{v'^2} - \overline{u'^2} \right) - \frac{1}{r_{E \cos\phi}} \frac{\partial}{\partial \phi} \left(\overline{u'v'} \cos^2 \phi \right) + f \cos\phi \frac{1}{\rho} \frac{\partial}{\partial z} \left(\rho \frac{\overline{v'T'}}{\frac{\partial \overline{T}}{\partial z} + \frac{R\overline{T}}{c_p H}} \right) \tag{6}$$

The forcing is given by horizontal derivatives of the momentum fluxes and the vertical derivative of heat flux in relation to vertical stability. The radius of the earth is given by r_E, f is the Coriolis parameter and ρ is the density of air. A discussion of synoptic-scale and planetary-scale filtered EP flux divergence is appended as a supplementary.

Characteristics of the mean flow are determined by orographic forcing, thermal forcing and eddy forcing (Held

et al., 2002). Orographic and thermal forcing can be explained by potential vorticity (PV). Through the conservation of PV on isentropic surfaces the absolute vorticity must change if the depth of an atmospheric column changes, leading to displacement of air masses (e.g. Holton, 2004). Local heating or diabatic forcing has the potential to change the distribution of PV, since it is associated with changes in density of PV (Haynes and McIntyre, 1987). The large-scale eddy forcing is described above in terms of EP flux diagnostics. If changes are considered, only diabatic forcing and large-scale eddy forcing are relevant on decadal time scales. Thus, our two diagnostic approaches cover the relevant forcings of the mean flow.

We phenomenologically discuss the interaction between large-scale turbulence and the mean flow jointly with the diabatic heating terms related to large-scale turbulent and the mean advection. We want to explore, whether a transfer or conversion of heat energy between these scales of advection can be assumed through a relation to EP flux divergence anomalies. Since there is no direct mathematical framework between the 3D EP flux diagnostics and the analysis of thermodynamic heat advection, we follow a phenomenological approach. We discuss eddy-related terms of the 3D EP flux diagnostics in relation to large-scale turbulent advection terms and mean flow terms of the 3D EP flux diagnostics in relation to mean advection terms, respectively. The EP flux diagnostics describe the interaction of large-scale eddies and mean flow based on momentum fluxes and heat fluxes. The corresponding large-scale circulation features are related to the corresponding advection of heat as described by the analysis of the thermodynamic equation. Therefore, a physical relation between these two types of diagnostics exists. These interactions are discussed based on the observed climatology and trend of each term. In terms of climatology, we further discuss the relation of diabatic forcing and the general circulation from an observational point of view.

The diagnostic is applied to the observed climate of the last decades based on the ERA-Interim reanalysis data (Dee et al., 2011). The reanalysis is generated six-hourly by a T255 spectral model with 60 vertical levels up to 0.1 hPa. All diagnostic calculations are performed on a 2°×2° grid with daily data, which is feasible for the analysis of large-scale circulation features. Diabatic heating rates and corresponding advection terms are calculated as a vertical mass-weighted integral for the troposphere from 850 hPa up to 300 hPa. We do not aim at a full characterization of the whole atmospheric column and thus not on the mass balanced full energy budget. The focus is on the free, quasi-geostrophic troposphere, the advective processes there and the corresponding interaction between large-scale eddies and the time mean flow. The analysis is performed on a monthly time scale and thus with a monthly mean in Equations (2) to (6). In the following, "mean" always refers to this time scale. The corresponding deviations and covariance terms correspond to variability limited by the daily data and the monthly mean as well as by the 2° spatial resolution. Therefore, they correspond to atmospheric variability ranging from the large mesoscale and synoptical scale to planetary scales.

In the following sections, we first discuss the climatology of the mean circulation, the processes related to diabatic heating and the interaction between large-scale eddies and the mean flow in the North Atlantic, Arctic and Eurasian sector. After this characterization we discuss the long-term trends. Climatology and trends are based on the ERA-Interim time series of winters from 1979/1980 to 2015/2016. Significance of trends is determined with a Student's *t*-test. Crasemann et al. (2017) have shown that changes of circulation regimes over the North Atlantic and Eurasian region differ between early winter and late winter. According to this, we analyze the early winter (December and January) and late winter (February and March) separately. The results have been checked against an analysis of all four single months. No inconsistencies of the general results have been identified. Moreover, the climatology shows only marginal changes over the whole winter and is analyzed over the period from December to March.

3 Results

3.1 Climatology

Diabatic heating in winter is characterized by a general contrast between ocean and land. Figure 1d shows the diabatic heating rate calculated as residual according to Equation (2) and integrated between 850 hPa and 300 hPa. Even in this mid-tropospheric region, the ocean is a region of heat source, while the land areas act as a heat sink. According to well-known features of the general atmospheric circulation (Holton, 2004), energy sources at the boundary between mid-latitudes and the polar regions drive the direct circulation of the polar cell. Air is warmed around 60°N leading to the Icelandic surface low, rises and moves northward. The corresponding circulation features in 500 hPa over the Atlantic Oceans are shown in Figures 1a, 1b and 1c for the winter circulation. Over land, the circulation turns slightly southward as observed over the Eurasian continent in particular over the eastern part. The lack of solar radiation in winter leads to the cooling of continental regions. Therefore, diabatic forcing with warm oceans and cold continents coincides with more northward and more southward flows, respectively. The related stationary large-scale waves can either be diagnosed as deviations of the geopotential height field from its zonal mean in Figure 1b or are directly visible in terms of wind vectors in Figure 1c. These planetary waves are a combined result of the diabatic, orographic and eddy forcing (Held et al., 2002). There is a strong wave number 2 component with troughs at 70°W and 150°E, but around 50°E, there is a

weak secondary trough that indicates a weak higher wave number component. A wave number 2 corresponds well to the diabatic forcing with two continents and two oceans. The orographic forcing of the Rocky Mountains further intensifies this pattern, whereas the Ural Mountains spatially correspond to the secondary trough at 50°E. Overall, these basic climatological results correspond to well-known features of the atmospheric circulation.

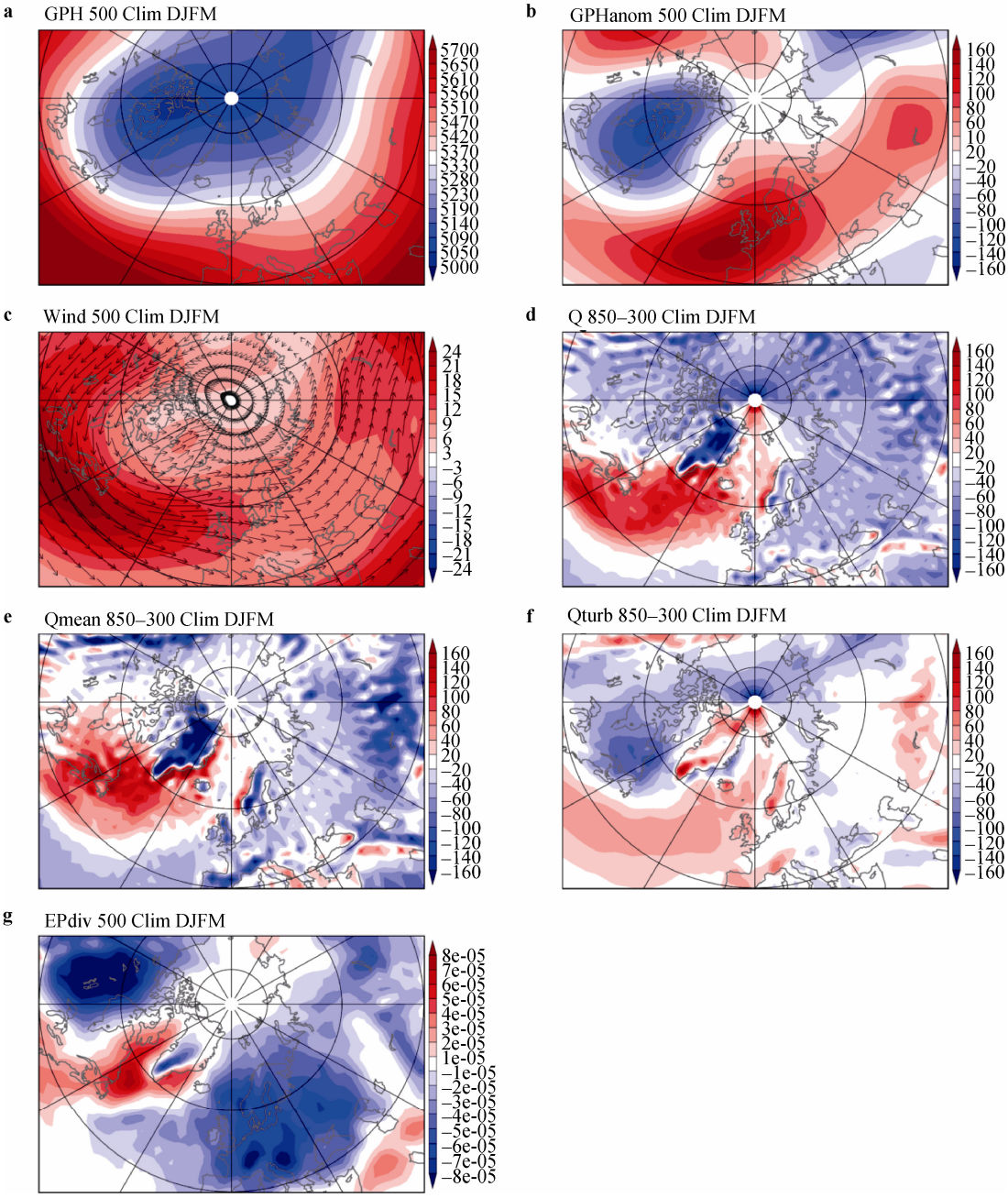

Figure 1 Winter (DJFM) Climatologies (1979–2016) of geopotential height in 500 hPa in m (**a**), geopotential height anomalies from zonal mean in 500 hPa in m (**b**), wind speed with wind vectors in 500 hPa in $m \cdot s^{-1}$ (**c**), diabatic heating rate integrated between 850 and 300 hPa in $W \cdot m^{-2}$ (**d**), mean heat advection integrated between 850 and 300 hPa in $W \cdot m^{-2}$ (**e**) and large-scale turbulent heat advection integrated between 850 and 300 hPa in $W \cdot m^{-2}$ (**f**), EP flux divergence in 500 hPa in $m \cdot s^{-2}$ (**g**).

Heat sources and the atmospheric circulation are directly related in terms of heat advection or more general in terms of energy transports. In Equation 2, two contributions to heat advection have been identified. The first contribution is the mean circulation involving monthly averages calculated according to Equation 5 and shown in Figure 1e. The other contribution to heat advection arises from the large-scale turbulent covariance terms, which is weaker in many regions. This term is calculated based on Equation 4 and shown in Figure 1f. These contributions are

discussed in the context of the diabatic heating rate estimated according to Equation 2 and shown in Figure 1d. A heat source exists over the ocean in winter. The atmospheric circulation gains heat and the resulting advection or transport is positive. Over land, a heat sink exists in winter, the atmospheric circulation loses or deposits heat and the advection or transport is negative. Over the central parts of ocean and land this is consistently reflected by mean and large-scale turbulent advection in Figures 1e and 1f, respectively.

In more detail, the climatological mean advection is positive over the eastern parts of the continents and becomes negative over the eastern parts of the oceans (Figure 1e). The large-scale turbulent advection is shifted towards the opposite direction (Figure 1f). This spatial phase shift between both terms can be interpreted as compensation between both types of advection in the regions of transition between ocean and land. We diagnosed a heat sink over land that is related to winter continental cooling. At the east coast of North America this is consistent with negative turbulent advection, which means, the atmosphere is losing heat here due to eddy-related processes. Mean advection is positive, which is not in agreement with the energy sink. It is assumed that this positive transport is driven from turbulent advection terms. Over the adjacent Atlantic Ocean we diagnose a source of heat that is consistent with positive mean advection transferring this energy into the atmosphere. Still the turbulent advection is negative and this heat is assumed to additionally drive the mean advection. At the west coast of Eurasia we have the opposite behavior, which is interpreted as a transfer of energy from mean advection to turbulent advection. These two regions of transition between ocean and continents are of particular interest for the EP flux diagnostics, since the interactions between quasi-stationary mean and large-scale turbulent flow can be analyzed in terms of EP flux divergence.

The ocean region in mid-latitudes is mostly characterized by strong westerlies as seen in Figure 1c that are related to intense storm tracks. Thus, the above described compensation mechanism can be related to the entrance and exit regions of storm tracks and the interaction between large-scale eddies and the mean flow. In general, the atmospheric circulation is driven by heat supply over the oceans (Hoskins and Valdes, 1990). Over the western parts, at the entrance region of the storm tracks, the contribution of large-scale turbulent advection is negative, while the mean advection is positive. The related interaction between large-scale eddies and the mean flow can be detected in the divergence of the 3D EP flux divergence in Figure 1g. It is positive in the same region of transition between North America and the Atlantic Ocean, which is the entrance region of the jet stream. Large-scale turbulent processes force the mean zonal wind component. As discussed before, related heat transports show a consistent behavior between negative large-scale turbulent advection and positive mean advection. This suggests an overall transfer of heat from large-scale turbulence to the mean flow. The sign of EP flux divergence is negative in most other regions. Here, the mean flow is slowed down by large-scale turbulence, which can also be interpreted as a forcing of turbulence by the mean flow related to atmospheric instabilities. Over the easternmost parts of the ocean and western parts of land, this coincides with negative mean heat advection, while the large-scale turbulent contribution is slightly positive. Therefore, we suggest a conversion of heat transport related to the mean flow to large-scale turbulent processes referring to the coherent findings based on heat advection and EP flux divergence. Over land, mean advection is in agreement with the energy sink of the cooling land through atmospheric heat loss, while large-scale turbulent advection is neutral. Through the observed compensation and negative EP flux divergence, it is indicated that the forcing of the large-scale turbulent transports originate from the mean advection. Large-scale turbulent systems have the potential to transfer heat deeper into the continents and into the Arctic, while the atmosphere is depositing heat to balance the heat sink that is basically related to missing solar radiation in winter. These general climatological features are the same over the Pacific region, but will not be further discussed there, while we are focusing on the region from North America over the North Atlantic and Arctic Ocean to Eurasia.

3.2 Trends

The changes in the time period from 1979 to 2016 of the climatological patterns of 500 hPa geopotential heights and winds shown in Figure 2 differ between the early winter season (December and January) and the late winter season (February and March). While higher geopotential heights are found in Arctic regions in the whole winter (Figures 2a and 2c) and the pressure gradient to the mid-latitudes is reduced accordingly (compare Figures 1a and 1b), the centers of significant change shift. In early winter, the strongest positive trend is found between Scandinavia and Siberia with a maximum above the Barents and Kara seas. A further significant increase of geopotential heights occurs over the easternmost part of North America. In late winter, the positive trend anomaly lies right over the central Arctic Ocean. Considering the climatological waviness of the geopotential height pattern in 500 hPa, we find two climatological troughs at 70°W and 150°E and a smaller one at 50°E according to Figure 1b. In all three regions, the anomaly patterns based on trends are different between the early and late winter trends. In early winter, these troughs are significantly filled (Figure 2a), while in late winter there is a weak deepening (Figure 2c). This indicates a straighter but also blocked flow in early winter, while in late winter the waviness and meridionalization is amplified.

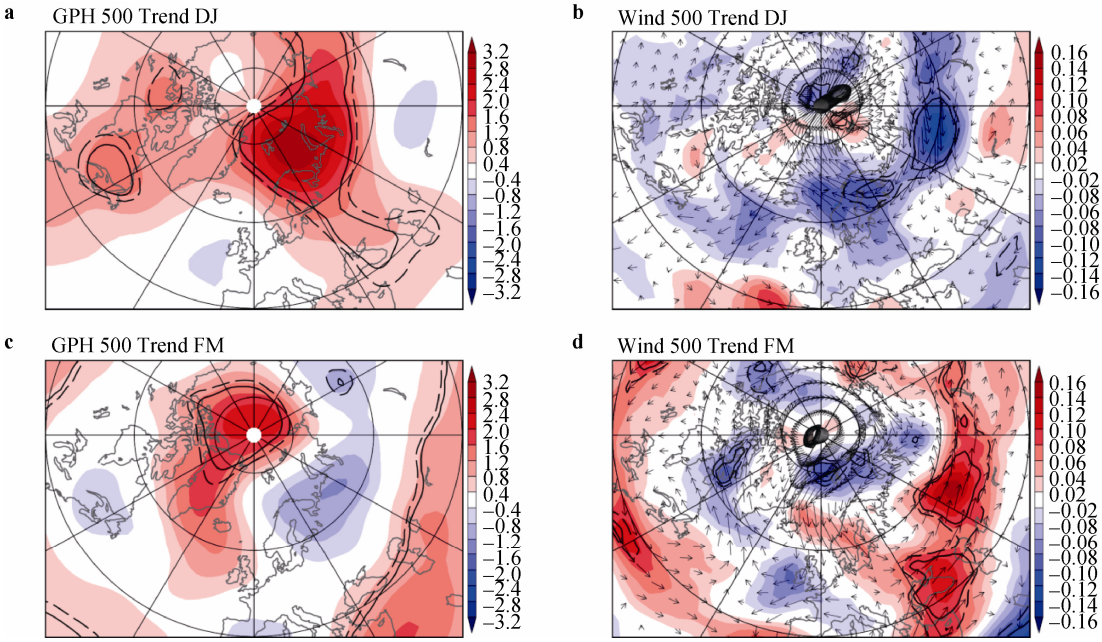

Figure 2 Trends (1979–2016) in DJ (**a**, **b**) and FM (**c**, **d**) of geopotential heights in $m \cdot a^{-1}$ (**a**, **c**) and wind speed with wind vectors in $m \cdot s^{-1} \cdot a^{-1}$ (**b**, **d**) both in 500 hPa. Significance at 95% (90%) level as solid (dashed) black contours.

The climatological westerly flow over the Atlantic in mid-latitudes is generally weaker in the whole winter mostly due to the reduced pressure gradient according to easterly wind trends in early winter (Figure 2b) and increasing meridional components in late winter (Figure 2d). In contrast, the circulation trend is reversed in the Arctic and over large parts of Eurasia between early and late winter as shown in Figures 2b and 2d. In more detail, the climatological circulation is weakened through anomalous easterly winds over the Atlantic Ocean roughly between North America and Island in early winter (Figure 2b). Northeast of this region, the trends show intensified southerly winds that transport warm air masses from the Atlantic Ocean into the Arctic. Consistent with higher geopotential heights indicating blocking, the wind magnitude is overall smaller, but the anomalous vectors show a clear northward trend. The anomalous flow then turns towards the Siberian Arctic, bringing polar air masses to the continent. Over the continent the flow is significantly reduced, which is again related to increasing geopotential heights. In late winter, the circulation over the North Atlantic and Arctic region is disturbed through trends with strong meridional components (Figure 2d). Thereby, the maritime influence from the Atlantic Ocean on European mid-latitudes is reduced. This is supported by an easterly wind trend over Western Europe. In more southern regions of the North Atlantic mid-latitudes, increased westerly winds are found indicating a southward shift of the wind maximum. Between Iceland, Scandinavia and the Arctic, wind trends have a similar high magnitude during the whole winter as indicated by the length of the vector, but point in the opposite direction. In the central Arctic, winds become calmer in agreement with the increasing geopotential heights in late winter (Figures 2c and 2d). Furthermore, anomalous winds arise from the Arctic and head towards Europe. Thus, the influence of the Arctic on Europe through northerly winds increases, which is different from early winter. In the continental Eurasian region, the trends intensify the climatological westerlies in late winter, which is also in contrast to early winter conditions.

The trend in mean winds certainly influences the mean advection terms. In early winter, we find negative trends of mean advection around the Scandinavian region extending well into the Arctic (Figure 3a). The atmosphere is depositing more heat stemming from the ocean in the south. This is in agreement with the intensified northward circulation as discussed before that reaches farther into the Arctic (compare Figure 2b). At the same time and in the same region, the trend of large-scale turbulent advection terms is positive as displayed in Figure 3b. This indicates the same compensation mechanism that we already suggested based on the climatological advection terms over the eastern boundaries of the oceans. Thus, the North Atlantic and the Arctic are strongly influenced by maritime conditions. More heat is transported here by the mean flow, acting as a potential source for additional large-scale turbulent heat advection. Further south and east over Siberia, both terms switch signs. These trends act against the climatological heat advection, which is in agreement with reduced westerly winds and weaker meridional gradients. The trends indicate a calmer and even more continental climate.

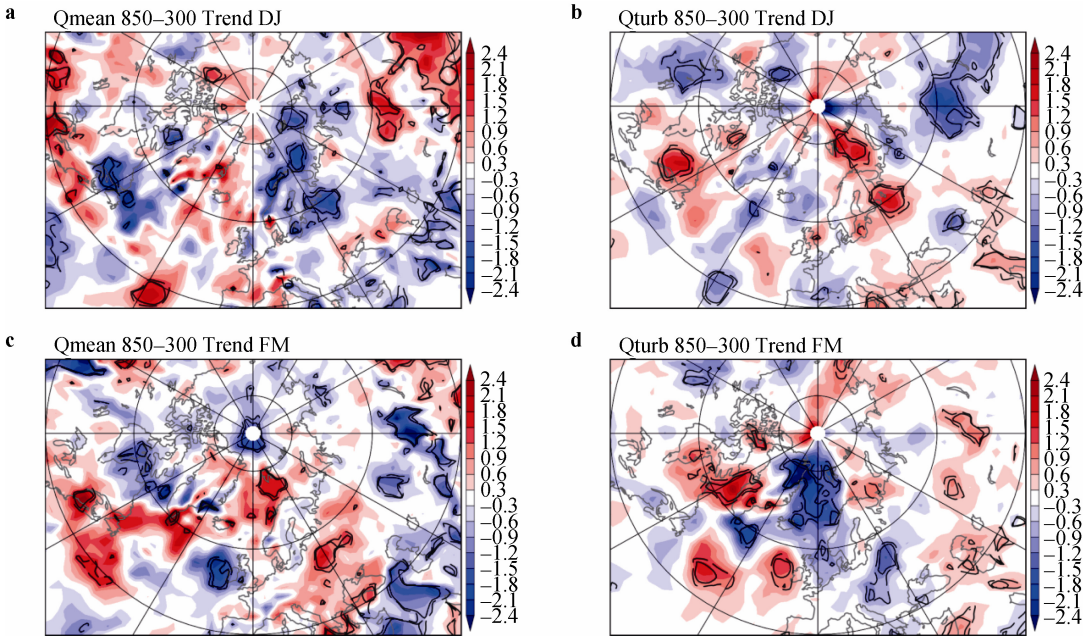

Figure 3 Trends (1979–2016) in DJ (**a**, **b**) and FM (**c**, **d**) of mean heat advection (**a**, **c**) and large-scale turbulent heat advection (**b**, **d**) both in $W \cdot m^{-2} \cdot a^{-1}$ and integrated between 850 hPa and 300 hPa. Significance at 95% (90%) level as solid (dashed) black contours.

The compensation of reduced mean and increased large-scale turbulent advection can be related to higher geopotential heights in the same region. Besides the Scandinavian region, this is also found in the very east of North America in early winter as displayed in Figures 3a and 3b. The reduction of mean advection corresponds to a blocking effect of the higher geopotential heights. The increase in large-scale turbulent advection could also be related to blocking, since it counteracts the climatological pattern as the mean advection does. This is true for the more continental anomalies over North America and east of Scandinavia. The anomalies over west and north of Scandinavia are in agreement with the higher geopotential heights in terms of forced southerly winds due to the intensified geopotential height gradient. This results in more maritime influence as discussed before. The anomaly at the eastern part of North America relates to interactions between large-scale eddies and the mean flow, which will be discussed later in more detail. Southwest of the negative North American anomaly of mean advection terms in Figure 3a, some further positive anomalies are found, which may indicate a shift of centers of action related to shifting jet streams.

In late winter, the compensating effects between mean and large-scale turbulent advection continue. Nevertheless, the trends are typically shifted or even inverted and show very different characteristics (Figures 3c and 3d) compared to early winter (Figures 3a and 3b). This corresponds well to the mostly reversed circulation trends that have been diagnosed before and were displayed in Figure 2. Figure 3c indicates positive trends of mean heat advection in the North Atlantic region. In a region of climatological neutral mean heat advection, these are explained by either less heat loss due to reduced northward transports or more heat supply related to anomalous southward flow of air (compare Figure 2d). Furthermore, weaker winds transport less heat into the Arctic, reducing the maritime influence. This is suggested by pronounced corresponding negative trends in terms of large-scale turbulent heat advection as displayed in Figure 3d. The influence from the intensified meridional flow leads to the alternating patterns of positive and negative trends starting over North America and continuing over the Atlantic Ocean. Still, these show signs of compensating each other with respect to mean and large-scale turbulent advection. The anomalous trends tend to reduce the climatological pattern except for the very western boundary of the Atlantic Ocean. This is related to intensified interaction between large-scale eddies and the mean flow, which will be discussed later. Over the southern parts of Siberia, the trends intensify the climatological pattern with stronger negative mean heat advection and enhanced positive large-scale turbulent heat advection. This is in agreement with the intensified climatological westerlies.

The trends of EP flux divergence are shown in Figure 4. Significance of EP flux divergence trends is generally patchy, but anomalies discussed here are in agreement with the trends discussed before, which implies robustness, although only small areas are significant. Trends of the EP flux divergence pattern are approximately inversed between early and late winter showing completely different characteristics of changes of the interaction between large-scale eddies and the mean flow in both periods. In

early winter (Figure 4a), the most striking feature is a weakening of the climatological EP flux divergence that starts in the eastern part of North America with negative trends and continues over the North Atlantic with positive trends. This weakening of the climatological pattern was already observed for the heat advection trends (Figures 3a and 3b). In this way, it can be suggested that the heat transfer from large-scale turbulence to the mean flow at the entrance of the storm track is reduced, which is consistent with weaker westerlies and weaker meridional gradients. The negative EP flux divergence trend anomaly at 70°E in early winter (Figure 4a) has a similar effect. In this region, the zonal wind is also reduced (Figure 2b). In the region with the strongest wind reduction east of this EP flux divergence anomaly, the positive trend of mean heat advection acts against negative climatological values as well (compare Figures 3a and 1e). An overall smoothing of the climatological pattern is induced by the trends over the Eurasian continent that is further indicated by the positive EP flux divergence anomaly at 30°E close to the region with the strongest climatological negative values. All features described here indicate increasingly calmer conditions. These have a potential relation to the positive geopotential height trends in between mid and high latitudes suppressing strong atmospheric flows and interaction between large-scale eddies and the mean flow.

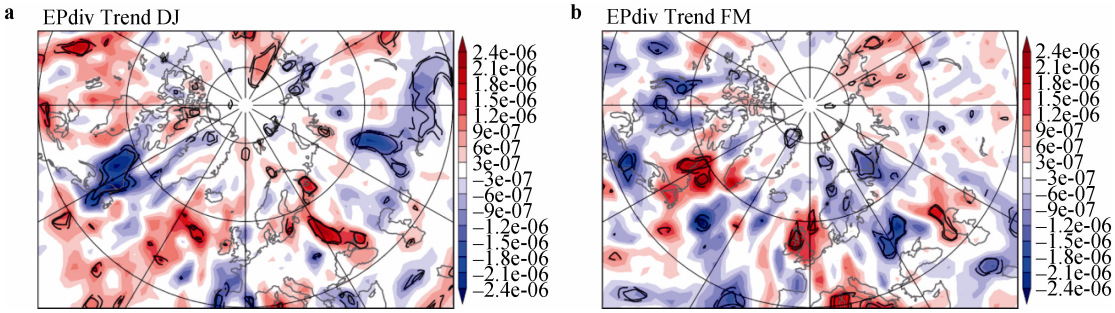

Figure 4 Trends (1979–2016) in DJ (**a**) and FM (**b**) of EP flux divergence in $m \cdot s^{-2} \cdot a^{-1}$ in 500 hPa. Significance at 95% (90%) level as solid (dashed) black contours.

In contrast, there is an intensification of the climatological EP flux divergence through the late winter trends at the westernmost part of the Atlantic Ocean (Figure 4b). In this specific region, it agrees with the observed forcing of mean advection and reduced large-scale turbulent terms. Again, the trend anomalies alternate further downstream in zonal direction. This is related to the occurrence of a more disturbed and meridional flow in late winter. The strong positive westerly wind trend over Eurasia is not conclusively related to any anomalies of EP flux divergence or heat advection. Especially over central Siberia we conclude that the interaction between mean flow and large-scale turbulence plays no role for this wind increase and is also not influenced by it.

4 Discussion and conclusions

The climatology and trends of advective components of the atmospheric heat energy budget and their relation to interactions between large-scale eddies and the mean flow have been analyzed in winter for the ERA-Interim period from 1979 to 2016. A fundamental feature is the strong contrasts between ocean and land. In winter, the ocean acts as a heat source, while the continents act as heat sink. This observation holds for large regions, if heat advection is separated into its mean contribution and the contribution of large-scale turbulent processes. Advection transports heat either away from sources or to sinks. A phase shift between the two contributions in the region of transition between continents and oceans indicates compensation and interaction. While mean advection is shifted westward, large-scale turbulent advection is shifted eastward relative to the ocean and land distribution. On the western boundary of the ocean, large-scale turbulent terms are negative and mean terms are positive, while the inverse situation occurs at the eastern boundary. These compensation effects are related to interactions between large-scale eddies and the mean flow. Starting at the western boundary of the ocean, atmospheric eddies force the strong mean flow and thus strong mean heat advection. This is diagnosed in terms of a positive 3D EP flux divergence. The relation is built on a phenomenological observation of corresponding anomalies of heat advection related to large-scale turbulence and the mean flow. Further downstream the flow becomes more turbulent, which is related to the storm tracks. The divergence of EP flux becomes negative indicating a forcing of eddies from the mean flow. Accordingly, the mean heat advection decreases and becomes negative while large-scale turbulent heat advection is still positive. This indicates a transition of transports related to quasi-stationary mean flow conditions to large-scale turbulent flow conditions that are consistent with negative EP flux divergence.

Changes of the advective contributions feature an additional compensation effect. If a positive trend of mean advection is diagnosed, a negative trend of large-scale turbulent advection is often found in the same region. Heat transports from heat advection are not overall increased or reduced. The findings suggest a change from the more

variable large-scale turbulent advection to the more stationary mean advection and vice versa. Inverse trends of both contributions to heat advection appear in several regions. These compensating effects are in agreement with the compensating effects in the climatology in transition regions and often counteract or amplify them.

Synoptic-scale and planetary-scale contributions of the large-scale turbulent terms can be separated, which is discussed in the supplementary material. Summarizing, both scales are in agreement in terms of significant trends almost everywhere, but the planetary-scale dominates concerning the magnitude of these trends. Therefore, a separation of scales does not add further insights to the general conclusions.

A general observation is the weakening of the zonal flow in the middle troposphere in mid-latitudes that is related to the trend of higher geopotential heights in high latitudes and the correspondingly reduced driving geopotential height gradient over the whole winter. In early winter, this is related to a reduced forcing of the Atlantic jet diagnosed in terms of reduced interactions between large-scale eddies and the mean flow. This further relates to the trend of positive geopotential height anomalies at the western and eastern transition between ocean and land over the Atlantic Ocean that also blocks the flow. The higher frequency of these conditions is confirmed by a preceding study by Crasemann et al. (2017). They find these blocking weather situations occurring more often during early winter in recent decades. Luo et al. (2016) also find a more persistent Ural blocking related to sea-ice loss in the Barents and Kara seas region and to the Warm Arctic – Cold Eurasia pattern. At the same time, the flow of air masses penetrates deeper into the Atlantic sector of the Arctic, in agreement with the western flank of the high anomaly over Scandinavia. This might be related to higher SSTs and the more positive phase of the AMO as well as reduced sea ice. These changes make the Arctic more maritime corresponding to more energy available in the north. The enhanced northward flow into the Arctic is confirmed by Dahlke and Maturilli (2017). The intensified anomalous flow of air into the Arctic cools there and enhances Siberian cooling when it penetrates back into the continent. If all early winter circulation anomalies together are taken into account, we find an overall more straight circulation with reduced higher wave numbers. The geopotential height ridge over the ocean is flattened and the weak climatological trough related to the Ural Mountains is filled. This is in agreement with EP flux divergence trends that smooth the corresponding climatological pattern.

Trends observed in early winter are reversed in late winter. Trends of heat advection components and EP flux divergence now intensify the climatological patterns in many regions. Furthermore, the geopotential height and circulation trends show a generally wavier pattern. The topic of meridionalization and intensification of large-scale waves was widely discussed in recent years. While some studies suggest an increase in waviness of the jet stream related to Arctic warming and weaker poleward gradients (Francis and Vavrus, 2012, 2015; Cattiaux et al., 2016), other studies discuss large uncertainties depending on the metrics that are implemented and pronounce strong interannual and decadal variability (Barnes, 2013; Screen and Simmonds, 2013). The intraseasonal variability between early and late winter described here, potentially explains the uncertainties in studies looking at the winter as a whole. We note that the reduction of the zonal flow consistently occurs in early and late winter over the Atlantic, although the mechanism is different. In late winter, the reduced westerlies are related to a wave-like forcing related to EP flux divergence and heat advection terms, which is in contrast to a reduced forcing and blocking highs observed in early winter.

The Arctic is directly influenced by a trend of increasing geopotential heights reducing the gradient to the mid-latitudes resembling a more negative AO phase in late winter. This is in agreement with a different approach by Crasemann et al. (2017), who detected an increased frequency of negative NAO conditions in late winter, that are closely related to the Atlantic impact of an negative phase of the AO. A negative AO phase is consistent with the trend of enhanced planetary waves and reduced or southward shifted zonal flow over the Atlantic. Consistent with this wavy structure of the flow, an anomalous flow from the Arctic towards Europe was detected, increasing the potential for cold events. This is supported by the intensified higher wave number anomalies in the geopotential height field and the deepened trough over Eastern Europe. Enhanced negative AO phases might be related to changes in the stratosphere in terms of downward propagating weak stratospheric polar vortex events according to Baldwin and Dunkerton (2001). This mechanism has been discussed with respect to sea ice changes in recent studies (Kim et al., 2014; Kretschmer et al., 2016; Jaiser et al., 2016). Thus, the anomalous trends in early winter are largely generated in the troposphere itself, while in late winter a stratospheric influence becomes more likely.

There are large consistencies between the findings provided by the study and previous studies as discussed before. This gives new insights to energy-related processes and further related interactions between large-scale turbulence and the mean flow. A clear attribution of these trends to specific changes, feedbacks or impacts is difficult. The diagnostic already is complex and rather sensitive, leading to the effect that extracting specific phenomena leads to diminishing statistical significance.

With this study, we introduced an improved set of diagnostics to determine the interaction of large-scale eddies and the mean flow in three-dimensional datasets and discuss their relation to diabatic processes based on a phenomenological approach. Since diabatic processes are very likely changing in a warming climate, this approach

contributes to a better process understanding in particular in studies involving future climate scenarios.

Acknowledgments This study has been supported by the project "QUAntifying Rapid Climate Change in the Arctic: regional feedbackS and large-scale impacts" (QUARCCS) funded by the German Federal Ministry for Education and Research (BMBF) under grant agreement 03F0777A and by the Helmholtz Climate Initiative REKLIM.

References

Andrews D G, McIntyre M E. 1976. Planetary waves in horizontal and vertical shear: The generalized Eliassen-Palm relation and the mean zonal acceleration. J Atmospheric Sci, 33(11): 2031-2048, doi: 10.1175/1520-0469(1976)033<2031:PWIHAV>2.0.CO;2.

Arguez A, O'Brien J J, Smith S R. 2009. Air temperature impacts over Eastern North America and Europe associated with low-frequency North Atlantic SST variability. Int J Climatol, 2009, 29(1): 1-10, doi: 10.1002/joc.1700.

Årthun M, Kolstad E W, Eldevik T, et al. 2018. Time scales and sources of European temperature variability. Geophys Res Lett, 45(8), doi: 10.1002/2018GL077401.

Baldwin M P, Dunkerton T J. 2001. Stratospheric harbingers of anomalous weather regimes. Science, 294(5542): 581-584, doi:10.1126/science. 1063315.

Barnes E A. 2013. Revisiting the evidence linking Arctic amplification to extreme weather in midlatitudes. Geophys Res Lett, 40(17): 4734-4739, doi:10.1002/grl.50880.

Barnes E A, Screen J A. 2015. The impact of Arctic warming on the midlatitude jet‐stream: Can it? Has it? Will it? Wiley Interdiscip Rev Clim Change, 6(3): 277-286, doi:10.1002/wcc.337.

Cattiaux J, Peings Y, Saint-Martin D, et al. 2016. Sinuosity of midlatitude atmospheric flow in a warming world. Geophys Res Lett, 43(15): 8259-8268, doi: 10.1002/2016GL070309.

Cohen J, Barlow M, Kushner P J, et al. 2007. Stratosphere–troposphere coupling and links with Eurasian land surface variability. J Climate, 20(21): 5335-5343, doi:10.1175/2007JCLI1725.1.

Cohen J, Screen J A, Furtado J C, et al. 2014. Recent Arctic amplification and extreme mid-latitude weather. Nat Geosci, 7(9): 627-637, doi: 10.1038/ngeo2234.

Crasemann B, Handorf D, Jaiser R, et al. 2017. Can preferred atmospheric circulation patterns over the North-Atlantic-Eurasian region be associated with arctic sea ice loss? Polar Sci, 14: 9-20, doi:10.1016/j.polar.2017.09.002.

Dahlke S, Maturilli M. 2017. Contribution of atmospheric advection to the amplified winter warming in the Arctic North Atlantic Region. Adv Meteorol, 2017: 1-8, doi:10.1155/2017/4928620.

Dee D P, Uppala S M, Simmons A J, et al. 2011. The ERA-Interim reanalysis: Configuration and performance of the data assimilation system. Q J Royal Meteorol Soc, 137(656): 553-597, doi:10.1002/qj.828.

Dethloff K, Grieger N, Schmitz G. 1987. Die transienten Eddy-Transporte in der Projektion auf die langen atmosphärischen Wellen auf der Basis des FGGE-Winters 1978/79. II: Die Transporte potentieller Vorticity. Zeitschrift für Meteorologie, 37(2): 69-84.

Edmon Jr H J, Hoskins B J, McIntyre M E. 1980. Eliassen-Palm cross sections for the troposphere. J Atmospheric Sci, 37(12): 2600-2616, doi: 10.1175/1520-0469(1980)037<2600:EPCSFT>2.0.CO;2.

Fletcher C G, Hardiman S C, Kushner P J, et al. 2009. The dynamical response to snow cover perturbations in a large ensemble of atmospheric GCM integrations. J Climate, 22(5): 1208-1222, doi:10.1175/2008JCLI2505.1.

Francis J A. 2017. Why are Arctic linkages to extreme weather still up in the air? Bull Am Meteorol Soc, 98(12): 2551-2557, doi:10.1175/BAMS-D-17-0006.1.

Francis J A, Vavrus S J. 2012. Evidence linking Arctic amplification to extreme weather in mid-latitudes. Geophys Res Lett, 39(6): L06801, doi: 10.1029/2012GL051000.

Francis J A, Vavrus S J. 2015. Evidence for a wavier jet stream in response to rapid Arctic warming. Environ Res Lett, 10(1): 014005, doi:10.1088/1748-9326/10/1/014005.

Furtado J C, Cohen J L, Tziperman E. 2016. The combined influences of autumnal snow and sea ice on Northern Hemisphere winters. Geophys Res Lett, 43(7): 3478-3485, doi: 10.1002/2016GL068108.

Gámiz-Fortis S R, Esteban-Parra M J, Pozo-Vázquez D, et al. 2011. Variability of the monthly European temperature and its association with the Atlantic sea-surface temperature from interannual to multidecadal scales. Int J Climatol, 31(14): 2115-2140, doi:10.1002/ joc.2219.

Gan B, Wu L. 2015. Feedbacks of sea surface temperature to wintertime storm tracks in the North Atlantic. J Climate, 28(1): 306-323, doi:10.1175/JCLI-D-13-00719.1.

Gastineau G, Frankignoul C. 2015. Influence of the North Atlantic SST variability on the atmospheric circulation during the twentieth century. J Climate, 28(4): 1396-1416, doi:10.1175/JCLI-D-14-00424.1.

Gastineau G, García-Serrano J, Frankignoul C. 2017. The influence of autumnal Eurasian snow cover on climate and its link with Arctic sea ice cover. J Climate, 30(19): 7599-7619, doi:10.1175/JCLI-D-16-0623.1.

Graham R M, Cohen L, Petty A A, et al. 2017. Increasing frequency and duration of Arctic winter warming events. Geophys Res Lett, 44(13): 6974-6983, doi:10.1002/2017GL073395.

Grosfeld K, Lohmann G, Rimbu N. 2008. The impact of Atlantic and Pacific Ocean sea surface temperature anomalies on the North Atlantic multidecadal variability. Tellus A, 60(4): 728-741, doi:10.1111/j.1600-0870.2008.00304.x.

Haynes P H, McIntyre M E. 1987. On the evolution of vorticity and potential vorticity in the presence of diabatic heating and frictional or other forces. J Atmospheric Sci, 44(5): 828-841, doi: 10.1175/1520-0469(1987)044<0828:OTEOVA>2.0.CO;2.

Held I M, Ting M, Wang H. 2002. Northern winter stationary waves: Theory and modeling. J Climate, 15(16): 2125-2144, doi: 10.1175/1520-0442(2002)015<2125:NWSWTA>2.0.CO;2.

Holton J R. 2004. An introduction to dynamic meteorology. Fourth Edition. Burlington: Academic Press, 88.

Hoskins B J, James I N, White G H. 1983. The shape, propagation and mean-flow interaction of large-scale weather systems. J Atmospheric Sci, 40(7): 1595-1612, doi: 10.1175/1520-0469(1983)040<1595: TSPAMF>2.0.CO;2.

Hoskins B J, Valdes P J. 1990. On the existence of storm-tracks. J Atmospheric Sci, 47(15): 1854-1864, doi: 10.1175/1520-0469(1990)

047<1854:OTEOST>2.0.CO;2.

Jaiser R, Dethloff K, Handorf D, et al. 2012. Impact of sea ice cover changes on the Northern Hemisphere atmospheric winter circulation. Tellus A, 64(1): 11595, doi:10.3402/tellusa.v64i0.11595.

Jaiser R, Dethloff K, Handorf D. 2013. Stratospheric response to Arctic sea ice retreat and associated planetary wave propagation changes. Tellus A, 65(1): 19375, doi:10.3402/tellusa.v65i0.19375.

Jaiser R, Nakamura T, Handorf D, et al. 2016. Atmospheric winter response to Arctic sea ice changes in reanalysis data and model simulations. J Geophys Res Atmos, 121(13): 7564-7577, doi:10.1002/2015JD024679.

Kim B M, Son S W, Min S K, et al. 2014. Weakening of the stratospheric polar vortex by Arctic sea-ice loss. Nat Commun, 5: 4646, doi:10.1038/ncomms5646.

Kretschmer M, Coumou D, Donges J F, et al. 2016. Using causal effect networks to analyze different Arctic drivers of midlatitude winter circulation. J Climate, 29(11): 4069-4081, doi:10.1175/JCLI-D-15-0654.1.

Kushnir Y, Robinson W A, Bladé I, et al. 2002. Atmospheric GCM response to extratropical SST anomalies: Synthesis and evaluation. J Climate, 15(16): 2233-2256, doi: 10.1175/1520-0442(2002)015<2233:AGRTES>2.0.CO;2.

Liu J, Curry J A, Wang H, et al. 2012. Impact of declining Arctic sea ice on winter snowfall. Proc Natl Acad Sci USA, 109(11): 4074-4079, doi:10.1073/pnas.1114910109.

Luo D, Xiao Y, Yao Y, et al. 2016. Impact of Ural blocking on winter warm Arctic–cold Eurasian anomalies. Part I: Blocking-induced amplification. J Climate, 29(11): 3925-3947, doi:10.1175/JCLI-D-15-0611.1.

McCusker K E, Kushner P J, Fyfe J C, et al. 2017. Remarkable separability of circulation response to Arctic sea ice loss and greenhouse gas forcing. Geophys Res Lett, 44: 7955-7964, doi:10.1002/2017GL074327.

Osborne J M, Screen J A, Collins M. 2017. Ocean–atmosphere state dependence of the atmospheric response to Arctic sea ice loss. J Climate, 30(5): 1537-1552, doi:10.1175/JCLI-D-16-0531.1.

Overland J, Francis J A, Hall R, et al. 2015. The melting Arctic and midlatitude weather patterns: Are they connected? J Climate, 28(20): 7917-7932, doi:10.1175/JCLI-D-14-00822.1.

Overland J E, Dethloff K, Francis J A, et al. 2016. Nonlinear response of mid-latitude weather to the changing Arctic. Nat Clim Change, 6(11): 992-999, doi:10.1038/nclimate3121.

Pachauri R K, Allen M R, Barros V R, et al. 2014. Climate Change 2014: Synthesis Report. Contribution of Working Groups I, II and III to the Fifth Assessment Report of the Intergovernmental Panel on Climate Change. IPCC, Geneva, Switzerland, 151.

Peings Y, Saint-Martin D, Douville H. 2012. A numerical sensitivity study of the influence of Siberian snow on the northern annular mode. J Climate, 25(2): 592-607, doi:10.1175/JCLI-D-11-00038.1.

Plumb R A. 1985. On the three-dimensional propagation of stationary waves. J Atmospheric Sci, 42(3): 217-229, doi: 10.1175/1520-0469(1985)042<0217:OTTDPO>2.0.CO;2.

Plumb R A. 1986. Three-dimensional propagation of transient quasi-geostrophic eddies and its relationship with the eddy forcing of the time—mean flow. J Atmospheric Sci, 43(16): 1657-1678, doi: 10.1175/1520-0469(1986)043<1657:TDPOTQ>2.0.CO;2.

Rinke A, Maturilli M, Graham R M, et al. 2017. Extreme cyclone events in the Arctic: Wintertime variability and trends. Environ Res Lett, 12(9): 094006, doi:10.1088/1748-9326/aa7def.

Screen J A, Deser C, Smith D M, et al. 2018. Consistency and discrepancy in the atmospheric response to Arctic sea-ice loss across climate models. Nat Geosci, 11: 155-163, doi:10.1038/s41561-018-0059-y.

Screen J A, Simmonds I. 2013. Exploring links between Arctic amplification and mid-latitude weather. Geophys Res Lett, 40(5): 959-964, doi:10.1002/grl.50174.

Semmler T, Stulic L, Jung T, et al. 2016. Seasonal atmospheric responses to reduced Arctic sea ice in an ensemble of coupled model simulations. J Climate, 29(16): 5893-5913, doi:10.1175/JCLI-D-15-0586.1.

Smith D M, Dunstone N J, Scaife A A, et al. 2017. Atmospheric response to Arctic and Antarctic sea ice: The importance of ocean–atmosphere coupling and the background state. J Climate, 30: 4547-4565, doi:10.1175/JCLI-D-16-0564.1.

Stroeve J C, Serreze M C, Barrett A, et al. 2011. Attribution of recent changes in autumn cyclone associated precipitation in the Arctic. Tellus A, 63(4): 653-663, doi:10.1111/j.1600-0870.2011.00515.x.

Tang Q, Zhang X, Yang X, et al. 2013. Cold winter extremes in northern continents linked to Arctic sea ice loss. Environ Res Lett, 8(1): 014036, doi:10.1088/1748-9326/8/1/014036.

Trenberth K E. 1986. An assessment of the impact of transient eddies on the zonal flow during a blocking episode using localized Eliassen-Palm flux diagnostics. J Atmospheric Sci, 43(19): 2070-2087, doi:10.1175/1520-0469(1986)043<2070:AAOTIO>2.0.CO;2.

Trenberth K E, Smith L. 2009. The three dimensional structure of the atmospheric energy budget: methodology and evaluation. Clim Dyn, 32(7-8): 1065-1079, doi:10.1007/s00382-008-0389-3.

Tyrrell N L, Karpechko A Y, Räisänen P. 2018. The influence of Eurasian snow extent on the northern extratropical stratosphere in a QBO resolving model. J Geophys Res Atmos, 123(1): 315-328, doi:10.1002/2017JD027378.

Vihma T. 2014. Effects of Arctic sea ice decline on weather and climate: A review. Surv Geophys, 35(5): 1175-1214, doi:10.1007/s10712-014-9284-0.

Wegmann M, Orsolini Y, Vázquez M, et al. 2015. Arctic moisture source for Eurasian snow cover variations in autumn. Environ Res Lett, 10(5): 054015, doi:10.1088/1748-9326/10/5/054015.

Zhang P, Wo Y, Simpson I R, et al. 2018. A stratospheric pathway linking a colder Siberia to Barents-Kara Sea sea ice loss. Sci Adv, 4(7): EAAT6025, doi:10.1126/sciadv.aat6025.